Journal of Applied Biology & Biotechnology Vol. 11(4), pp. 164-169, Jul-Aug, 2023
Available online at http://www.jabonline.in
DOI: 10.7324/JABB.2023.11512

Biocompatibility of hydrophilic regenerated *Antheraea mylitta* silk fibroin

Shruti Dixit[1], Tilak Gasti[2], Ankith Sherapura[3], B. T. Prabhakar[3], Shyam Kumar Vootla[1]*

[1]Department of Microbiology and Biotechnology, Karnatak University, Pavate Nagar, Dharwad, Karnataka, India.
[2]Department of Chemistry, Khaja Bandanawaz University, Kalaburagi, Karnataka, India.
[3]Department of Studies and Research in Biotechnology, Sahyadri Science College (Autonomous), Kuvempu University, Shimoga, Karnataka, India.

ARTICLE INFO

Article history:
Received on: January 29, 2023
Accepted on: April 18, 2023
Available online: June 04, 2023

Key words:
Antheraea mylitta,
Silk fibroin,
Calcium nitrate tetrahydrate,
Biocompatibility,
Degummed silk fibers.

ABSTRACT

Silk, a natural biopolymer, is used for both textile and biomedical applications. Natural biopolymers are currently being used in various fields such as tissue engineering, wound healing, and food packaging based on their intrinsic qualities of safety, biocompatibility, and biodegradability, which make them the material of choice. Silk fibroin proteins from the *Antheraea mylitta* wild silkworm are the least studied in the field of biomaterials. The β-sheet structures found in non-mulberry silk fibroin protein improve its mechanical properties. The present study was undertaken to regenerate water-soluble *A. mylitta* silk fibroin to improve its applications and enhance fabrication efficiency. The silk fibroin was regenerated by dissolving degummed silk fibers in calcium nitrate tetrahydrate salt at 100°C for 3 h. The biophysical characterization of regenerated silk fibroin was carried out by X-ray diffraction, scanning electron microscope, Therapeutic Goods Administration, Fourier-transform infrared spectroscopy, and differential scanning calorimetry, confirming the indigenous aspects of the "regenerated silk fibroin (RSF)". CD spectra were employed to track α-helix to β-sheet conformational transition changes in RSF. MTT assays using NIH3T3 fibroblast cells revealed that the RSF exhibited no toxicity and resulted in the proliferation of cells.

1. INTRODUCTION

The biopolymers such as collagen, cellulose, chitosan, silk, keratin, and gelatin, which are available naturally, have become increasingly popular in recent decades [1]. The novel qualities such as non-toxicity, biocompatibility, and biodegradability that are present in natural biopolymers enable them to be preferred over synthetic ones in many different applications, such as tissue engineering, wound healing, and food packaging. Silk, a natural biopolymer produced by silkworms, is divided into two types: domestic (*Bombyx mori*) and wild (*A. mylitta, A. assamensis, P. ricini*, etc.). Silk fibroin was commonly preferred because it has toughness, biodegradability, and heat resistance [2]. The mulberry and non-mulberry silkworms have distinct differences in their amino acid and polypeptide sequences, resulting in some property variations. The amino acid sequences (RGD) present in non-mulberry silk fibroin include cell proliferation and cell attachment sites, making it remarkably biocompatible and a popular choice among researchers for biomedical applications [2]. The inherent hydrophilic, crystalline, and β-pleated structures result in the protein's insolubility in universal solvents such as water. The challenges of dissolving and processing non-mulberry silk fibroin have resulted in limited applications of fibroin in research. Many applications have previously utilized the gel form of silk fibroin produced in the silkworm gland. Silk fibroin extraction from silkworm glands is commercially unavailable [3].

In addition to other natural biomaterials, silk fibroin amino acid sequences contain over 90% alanine, serine, and glycine. Silk fibroin has been widely studied for its biomedical applications such as the remodeling of tissues, wound healing, and drug delivery, where it can be employed as a biomaterial, due to its complete biodegradability, biocompatibility, and mechanical characteristics [4]. Silks are appealing biomaterials due to their protein-based molecular structure, which provides high *in vivo* biocompatibility in the medical field [5]. The mechanical adaptability of silks may be advantageous in the fabrication of artificial teeth, blood arteries, and skin grafts. Silk fibroin is increasingly used as a surgical thread due to its superior mechanical and physical properties. Despite its superior biocompatibility, applications of silk fibroin have been limited due to the intrinsic biophysical orientation of amino acids, which makes dissolving and further processing non-mulberry silk fibroin difficult. Chaotropic salts such as lithium bromide and calcium chloride were used to destabilize the proteins in the solution before dissolving *B. mori* silk fibroin. Because of their high resistance to these chemicals, these salts have issues dissolving *A.mylitta* silk fibroin [6]. The primary appearance of *A.mylitta* silk fibroin is an antiparallel β-sheet structure with H-bonding chains through -NH and -C=O groups [7]. Silk fibroin derived from

*Corresponding Author:
Shyam Kumar Vootla,
Department of Microbiology and Biotechnology, Karnatak University, Pavatenagar, Dharwad - 580 003, Karnataka, India.
E-mail: vootlashyam @ kud.ac.in

A. mylitta is not completely dissolvable in the solvents often used to dissolve natural polymers [2]. To circumvent this, we dissolved silk fibers with non-toxic and biocompatible calcium nitrate tetrahydrate. The regenerated silk fibroin (RSF) was biophysically characterized to confirm its natural characteristics [8].

The concept of the study is to explore the properties of water-soluble RSF, as well as its characterization and its greatly effect on the structures observed in calcium nitrate tetrahydrate *A.mylitta* fibroin powder regenerated from cocoons. To characterize the biophysical properties of RSF, different characterization techniques have been employed. The biocompatibility and cytotoxicity of the RSF against NIH3T3 fibroblast cell lines were tested through MTT assay. This study aims to produce hydrophilic regenerated wild (*A. mylitta*) silk fibroin from cocoons, which will enhance its medicinal applications.

2. MATERIALS AND METHODS

2.1. Materials

The Regional Tasar Research Station in Warangal, Telangana, India, provided *A. mylitta* cocoons and will be used for protein extractions. Sigma supplied calcium nitrate tetrahydrate ($Ca(NO_3)_2 \cdot 4H_2O$) and sodium carbonate (Na_2CO_3). SERVAPORE® dialysis tube (MWCO 12-14 kDa) was selected to perform dialysis against demineralized water. NCCS, Pune, provided NIH3T3 fibroblast cell lines. Cell culture medium was prepared to contain DMEM -High Glucose (Sigma), Sigma-Aldrich (India) provided fetal bovine serum, 3-(4,5-dimethylthiazol-2)-2,5-diphenyltetrazolium bromide (MTT), DMSO, and PBS. 96-well plates for culturing of cells, CO_2 incubator.

2.2. Methods

2.2.1. Degumming of silk fibers

Degumming of *A. mylitta* cocoons was performed according to a previously established methodology [9]. The cocoons were weighed at around 10 g, sliced into minute pieces, and cooked for 1 h at 100°C in 250 mL of 0.02M Na_2CO_3 solution. Thereafter, the fibrous material was then treated three times for 20 min in 1 L of warm water before drying for 12 h. For fibroin extraction, these degummed silk fibers have been utilized [10].

2.2.2. Synthesis of dissolved and RSF

The resulting silk fibers were dissolved in calcium nitrate tetrahydrate salt (1:80) in an oil bath at 80°C for 6 h with constant slow stirring. The obtained solution was dialyzed against distilled water using pre-treated dialysis tubing, and the water was replenished at regular intervals for 3 days. Finally, freeze-drying or lyophilization (LABFREEZ FD-10 freeze drier) was utilized to keep the silk fibroin powder at room temperature for a longer period of time [11].

2.2.3. Scanning electron microscopy

A scanning electron microscope was employed to observe the morphological characteristics of the silk strand (JEOL J S M-I T 500). The silk fiber was vacuum coated with gold, and the scans were obtained at a resolution of 200m with a voltage of 15 kV.

2.2.4. Fourier transform–infrared–ATR spectroscopy

FT-IR ATR spectroscopy was performed on the degummed fiber and regenerated fibroin using a Nicolet iZ10, USA FT-IR-ATR spectrometer. The resolutions of the spectral bands ranged from 4000 to 400 cm-1 [12].

2.2.5. X-Ray Diffraction (XRD)

The XRD was employed to confirm the structure and analyze the crystallinity of both degummed silk fiber and RSF samples using a Japan SmartlabSE Cu-Kα radiation (λ1 - 5405980 nm) [13]. Scanning was performed between the angle (2θ) from 5 to 70° with an applying a current of 45 kV and a voltage of 40 mA [12].

2.2.6. Differential scanning calorimeter (DSC) measurement

The samples were subjected to DSC thermal scanning using the Universal V4.5ATA Instrument at a heating rate of 10°C/min^{-1} under a nitrogen atmosphere (50 mL/min^{-1}) between the temperature ranges from ambient temperature to 450°C [13].

2.2.7. Thermo gravimetric (TG) analysis

The samples were then subjected to TG analysis using the Universal V4.5 ATA Instrument at a heating rate of 10°C/min^{-1} under a nitrogen atmosphere (50 mL/min^{-1}) over the temperature ranges from room temperature to 450°C [13].

2.2.8. Circular dichroism spectroscopy

A J-815 CD spectrometer (JASCO, Japan) with a 1.0-mm path-length cell at 28°C, a 4 s accumulating time, and a scanning speed of 100 nm/min^{-1} was used to measure the ellipticity of RSF solutions containing 0.1 mg/mL^{-1}. Under the same conditions, a blank solution was measured and subtracted from the sample spectrum.

2.2.9. In vitro Cytotoxicity

To investigate the cytotoxicity of the samples, NIH3T3 fibroblast cells were cultured in 96-well culture plates at a density of 1×10^4 cells per well and were incubated at 37°C for 24 h. Thereafter, 10 µL of MTT was added every 24, 48, and 72 h with the replacement of new media and was incubated. Media containing only 10% FCS was used as a control [14].

A stock solution (100 µL/$well^{-1}$) was employed to disintegrate the formazan crystals which were developed in the cells. A microplate reader (Model 550) was employed to record the OD at 570 nm (Bio-Rad. Inc.). The relative growth rate was estimated using Eq. (1) and cytotoxicity grading parameters were applied to assess cytotoxicity [15].

$$RGR = \frac{\text{OD value of samples}}{\text{OD value of negative control}} \times 100 \quad (1)$$

3. RESULTS

3.1. Surface Morphology

Surface microstructural arrangement is essential in the development of any biomaterial that will be employed in tissue engineering. Scanning electron microscope was utilized to observe the surface morphology of both degummed silk fibers and native *A.mylitta* cocoons [Figure 1] [16]. The rough and aggregated look of natural undegummed silk fiber [Figure 2a] is clearly visible due to the presence of sericin, whereas total degumming [Figure 2b] is visible due to the complete removal of sericin. When compared to the intrinsic undegummed silk fibers, the surface microstructural arrangement of the degummed silk fibers indicated full elimination of the sericin [12].

3.2. Structural Properties

3.2.1. FT-IR spectroscopy

The characterization of the RSF was done using FT-IR for macromolecular conformation as shown in Figure 3. Structural conformation silk protein was concluded by observing absorption

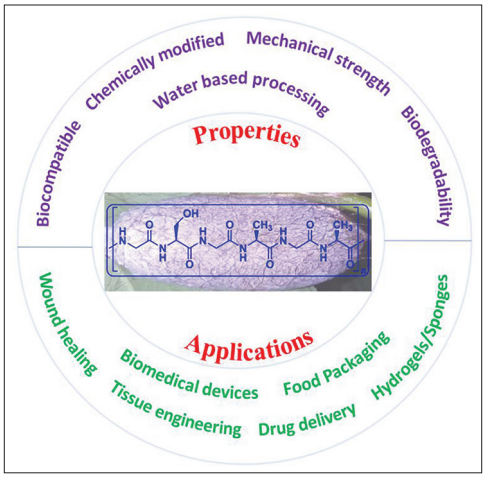

Figure 1: Structural properties and applications of silk fibroin.

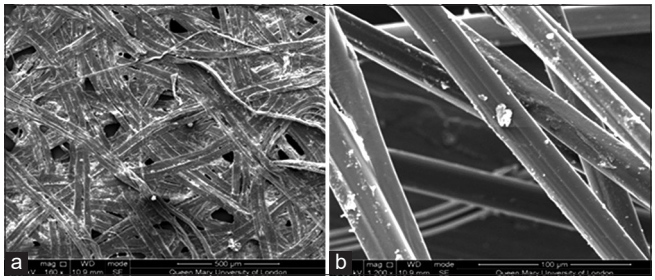

Figure 2: Surface microstructral behavior of (a) undegummed fiber and (b) degummed fiber.

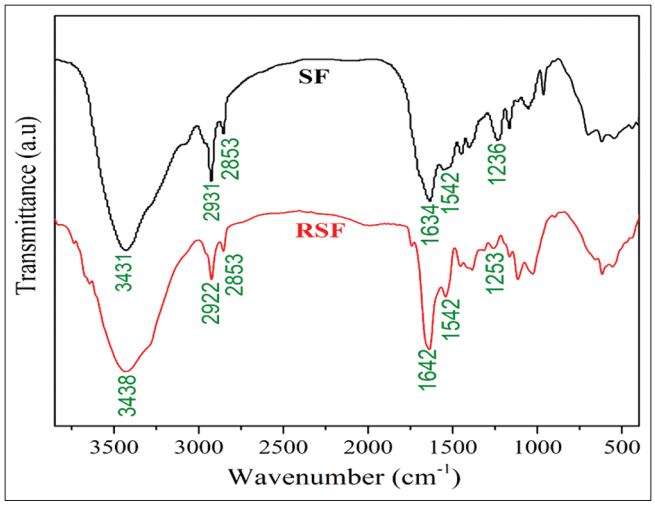

Figure 3: Fourier transform-infrared spectra of silk fibroin and regenerated silk fibroin.

bands of amide-I (1700–1600 cm^{-1}), amide-II (1600–1500 cm^{-1}), and amide-III (1300–1220 cm^{-1}) which are associated with the peptide chain [17]. The distinctive C=O stretching for amide-I at 1634 cm^{-1} was observed for degummed silk fibers in the spectra [18], it also showed secondary N–H bending at 1542 cm^{-1} for amide-II and at 1236 cm^{-1}, the presence of characteristic C–N stretching for amide-III was detected [19]. The RSF spectra showed a characteristic C=O stretching band at 1642 cm^{-1} for amide-I which is due to the β conformation, the secondary N–H bending band was seen at 1542 cm^{-1} for amide-II, which may be because of random coil conformation, whereas amide-III C–N stretching was observed at 1253 cm^{-1} [Figure 1 and Table 1]. The two absorption bands observed at 3438 and 2922 are due to the vibrations of the free OH and NH stretching, respectively [20].

3.2.2. X-ray diffraction

The secondary structure depicted by the FT-IR-ATR was further confirmed by the XRD studies. The XRD patterns of both degummed silk fibroin (SF) and RSF were examined to detect the variations in the crystalline structure. The XRD pattern helps to predict and confirm the α-helix and β-sheet structure with Cu Kα radiation [21]. The degummed silk fiber had a sharp β-sheet structure diffraction peak at 16.45 and 20.31, whereas the RSF had a high-crystalline β-sheet structure peak at 20.95°, as shown in Figure 4 below [22]. The XRD analysis showed similar crystalline structures as degummed fibers in RSF. XRD study proved that both RSF and degummed silk fibroin have β-sheet structures. The crystallinity structure of silk is determined by its β-sheet composition. The major peaks on the XRD curves of degummed fiber at 16.45° and 20.31° indicate an intense β-sheet structure. The diffraction peak in regenerated fibroin's β-sheet high crystalline structure is around 20.95°.

3.2.3. Differential scanning colorimetry

DSC instrumentation study was conducted to investigate the thermal capability of both degummed SF and RSF [Figure 5]. During the first run, two endothermic peaks were observed for the sample: the first is broader and centers at around 54°C for degummed silk fiber and 70°C for RSF, whereas the second is sharper and centers at approximately 360°C for both degummed silk fiber and RSF [23]. The β-sheet transition confirmation from random coil conformation could be attributed to higher temperature endothermic peaks, whereas the water loss observed in the DSC run was depicted by lower temperature endothermic peaks in Figure 5 [24].

3.2.4. Thermogravimetric analysis

The thermograms of degummed fiber and RSF are displayed in Figure 6. The samples RSF and degummed fibers showed initial weight loss at around 100°C, because of the evaporation of physically bonded water vapors from SF and RSF [25]. Both the samples exhibited almost similar moisture content. The Therapeutic Goods Administration (TGA) curves indicate that as temperature increased, the samples attained thermal stability up to 275°C, also depicting a sharp drop, indicating the initial thermal decomposition along with faster weight loss [26]. The second degradation occurred at 370°C for both degummed fiber and RSF. This significant breakdown resulted from both the breakage of the peptide link and the degradation of the remaining polymeric backbone of the amino group [26]. After a number of extraction techniques, the current study revealed that regenerated fibroin has the same thermal strength as degummed fiber [26]. TGA study corroborated the thermal stability of both degummed fiber and regenerated fibroin.

3.2.5. CD spectroscopy

A circular dichroism spectroscopy investigation further validated the RSF's structural modifications. The RSF sample's spectra revealed a negative band at 220 nm, indicating a β-sheet structure [27], and the shift from random coil to β-sheet form was evidenced in RSF's structural conformation [28]. The presence of β-sheet structure in the RSF was revealed by CD spectra [Figure 7].

3.2.6. Cell toxicity

Silk fibroin, as a potential wound dressing material, should encourage cell proliferation and differentiation. MTT assays were utilized

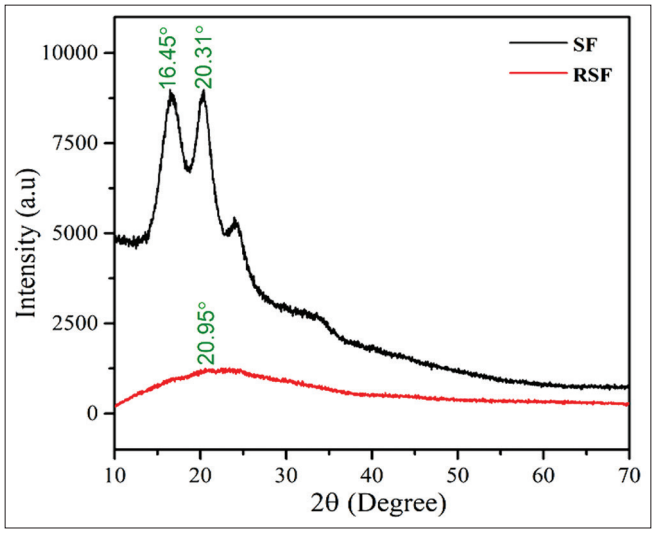

Figure 4: X-ray diffraction patterns silk fibroin and regenerated silk fibroin.

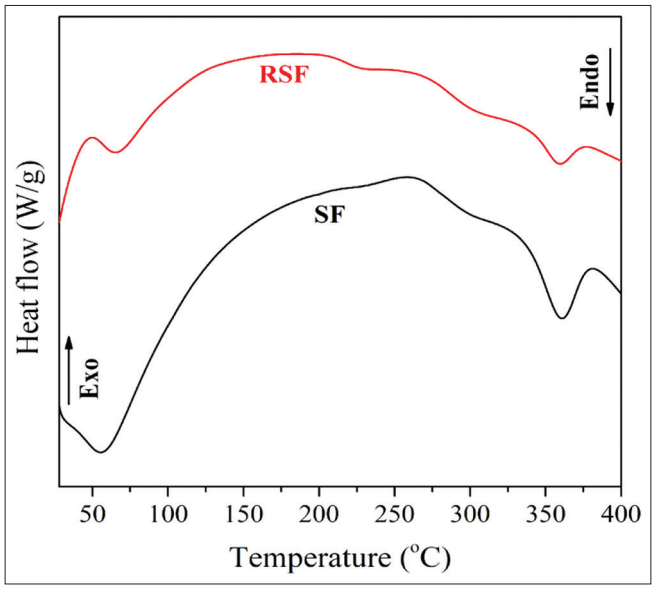

Figure 5: Differential scanning calorimeter thermograms of silk fibroin and regenerated silk fibroin.

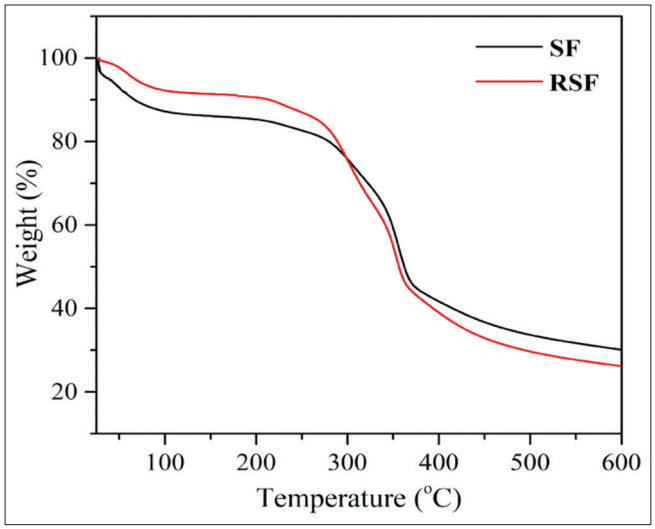

Figure 6: Thermogravimetric curves of silk fibroin and regenerated silk fibroin.

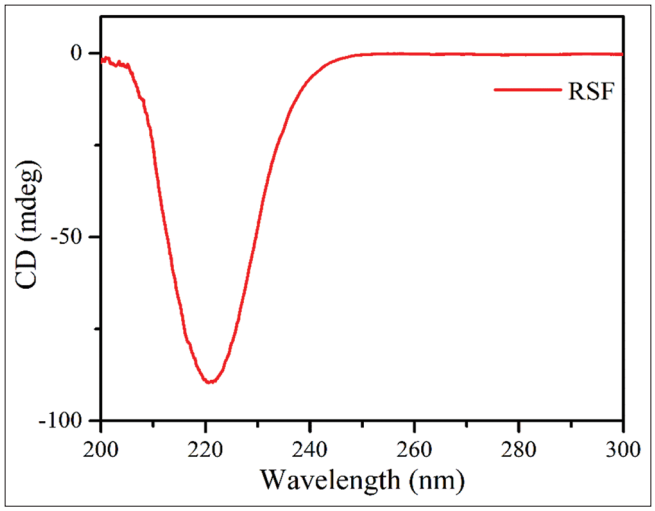

Figure 7: CD spectrum of regenerated silk fibroin.

to analyze the *in vitro* cytotoxicity of silk fibroin against NIH3T3 fibroblast cell lines [29]. The cell viability at 24, 48, and 72 h was over 80% for all concentrations up to 100 µg/mL, demonstrating silk fibroin's non-toxic and high bio-compatibility with cells [30]. This finding showed that the silk fibroin not only had high bio-compatibility but also had a favorable effect on cell growth, proving its biocompatibility properties [31]. The cell toxicity findings [Figure 8] indicate that the regenerated *A. mylitta* silk fibroin is non-toxic and has the potential to be advantageous in biomedical applications.

4. DISCUSSION

The degummed silk fibers' surface morphology exhibited entire eradication of sericin as compared to the natural undegummed silk fibers [12]. FT-IR corroborated the β-sheet structures of *A. mylitta* degummed silk and RSF. The existence of amide groups is responsible for the attribute amide-I (C=O stretching) in silk proteins, which gave a distinct vibration band around (1700–1600 cm^{-1}), whereas amide-II (N-H bending) bands were observed around (1600–1500 cm1), and amide-III (C-N stretching) bands were observed around (1300–1200 cm^{-1}) [17]. The existence of a hydrogen-bonding NH group was depicted by these all-characteristic absorbance peaks. The RSF's FT-IR spectra revealed significant absorption peaks at 1642, 1542, and 1253 cm^{-1} [20].

The β-sheet structure of both RSF and degummed fiber was validated by XRD. The silk fibroin's crystallinity is affected by β-sheet composition. The intense peaks on the XRD curves of degummed fiber at 16.45° and 20.31° indicate an intense β-sheet structure [21]. In regenerated fibroin, the β-sheet high-crystalline structure was noticed, with a diffraction peak at 20.95° [22]. RSF is thought to have slightly less crystallinity than raw SF. This result shows that the calcium nitrate treatment did not affect the SF's β-sheet structure. This result is largely in line with the earlier study. [32]. On the other hand, the DSC studies revealed that the minimum thermal decomposition temperature for degummed silk fiber is at 54 °C and for RSF is at 70 °C. The increase or decrease in thermal degradation may be due to specific preparation procedures and thermal treatment [23]. Furthermore, the accumulation

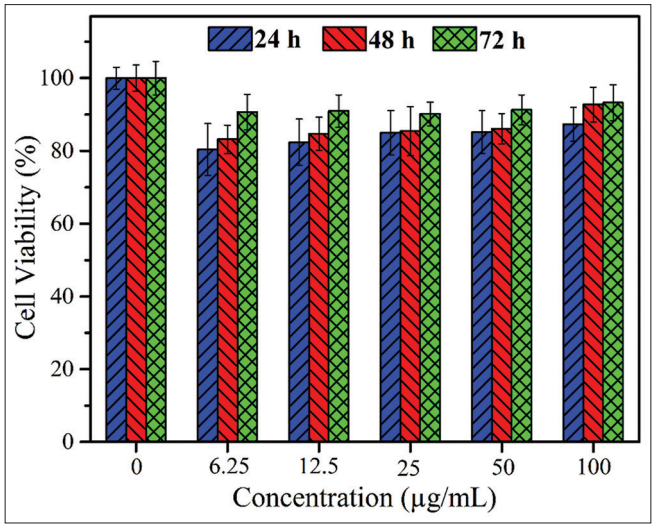

Figure 8: Cell toxicity of regenerated silk fibroin.

Table 1: Adsorption band positions of Degummed fibers and RSF.

Absorption band	Wavenumber (cm^{-1})	
	Degummed fibers	RSF
Amide–I	1634 cm^{-1}	1642 cm^{-1}
Amide–II	1542 cm^{-1}	1542 cm^{-1}
Amide–III	1236 cm^{-1}	1253 cm^{-1}

RSF: Regenerated silk fibroin

of Ca atoms on the SF caused a shift in the endothermic peak of the RSF. These findings are consistent with previously reported DSC plots of sodium carbonate regenerated SF [33].

Both degummed fiber and regenerated fibroin retained their thermal stability which was confirmed by TGA analysis. CD spectra revealed the existence of β-sheet structure in the RSF [28]. The cytotoxicity of the RSF revealed maximum cell viability because *A. mylitta* silk fibroin has a larger amount of glycine, which enhances cell adhesion and cell growth of L929 fibroblast cells. These results are consistent with the earlier reports [12,34,35]. The regenerated silk fiber seems to have higher thermal stability than the degummed fiber after a sequence of extraction processes. The findings suggested that the regenerated fibroin has more crystalline regions (β-sheets) than the other, which can increase the stability of drugs or therapeutic proteins, hence improving their activity [26]. The qualities of RSF met the demands of the current materials, leaving behind the synthetic polymer materials that have been used for decades.

Dissolvable stitches, devices for drug delivery, and fiber-based tissue devices that make use of silk proteins' mechanical characteristics will be developed in the future and may be employed for ligament and bone repairs; they may become increasingly common in the future [29]. Silk-based materials have the potential to develop a multifunctional material platform that integrates with the biological system in health care and commercial applications [31].

5. CONCLUSIONS

Our findings support the idea that biophysical characteristics and protein conformation are connected. According to FT-IR studies, the material's structure was primarily random coil conformation with a β-sheet structure. An XRD study revealed the crystallinity of the RSF. The TGA study exhibited remarkable thermal stability. The RSF's conformational changes from random coil to β-sheet form were revealed utilizing CD spectra. The MTT results also showed that the silk fibroin not only had high biocompatibility but also had a favorable effect on cell growth, revealing that it is a good biomaterial. The findings suggested that the regenerated fibroin has more crystalline regions (β-sheets) than the other, which can increase the stability of drugs or therapeutic proteins, hence improving their activity. The qualities of RSF met the demands of current materials used, leaving behind the synthetic polymer materials which are being used for decades and can be used as a biomaterial in the field of tissue engineering, wound healing, etc.

6. ACKNOWLEDGMENTS

The authors sincerely acknowledge KSTePS VGST-CISEE project number KSTePS/Grant/CISEE/GRD.No.932/2020-21/76 for funding this work. The authors also acknowledge DST–(PURSE – II), DST-SAIF, and University Scientific Instrumentation Center (USIC) Karnatak University, Dharwad, for providing necessary facilities.

7. AUTHORS' CONTRIBUTIONS

SD: Conceptualization; Data duration; Formal analysis; Methodology; Resources; Roles: Writing – Original draft; TG: Software; Resources; Investigation; Writing – original draft. AS and PBT: Methodology; Formal analysis; Role: Writing –Review & editing, SKV: Corresponding author; Resources; Formal analysis; Validation; Supervision, Project administrator, Role: Writing – Review and editing.

8. CONFLICTS OF INTEREST

The authors report no financial or any other conflicts of interest in this work.

9. ETHICAL APPROVALS

This study does not involve experiments on animals or human subjects.

10. DATA AVAILABILITY

All the related data are included in this published article.

11. PUBLISHER'S NOTE

This journal remains neutral with regard to jurisdictional claims in published institutional affiliation.

REFERENCES

1. Wu R, Li H, Yang Y, Zheng Q, Li S, Chen Y. Bioactive silk fibroin-based hybrid biomaterials for musculoskeletal engineering: Recent progress and perspectives. ACS Appl Bio Mater 2021;4:6630-46.
2. Batra R, Purwar R. Deduction of a facile method to construct *Antheraea mylitta* silk fibroin/gelatin blend films for prospective biomedical applications. Polym Int 2021;70:73-82.
3. Nguyen TP, Nguyen QV, Nguyen VH, Le TH, Huynh VQ, Vo DV, *et al*. Silk fibroin-based biomaterials for biomedical applications: A review. Polymers 2019;11:1933.
4. Hasan A, Abdel-Raouf ME. Cellulose-based superabsorbent hydrogels. In: Polymers and Polymeric Composites: A Reference

Series. Cham: Springer International Publishing; 2019.
5. Bunning TJ, Jiang H, Adams WW, Crane RL, Farmer B, Kaplan D. Applications of Silk. Washington, D.C.: ACS Publications; 1993. p. 353-8.
6. Ha SW, Park YH, Hudson SM. Dissolution of *Bombyx mori* silk fibroin in the calcium nitrate tetrahydrate-methanol system and aspects of wet spinning of fibroin solution. Biomacromolecules 2003;4:488-96.
7. Um IC, Kweon H, Park YH, Hudson S. Structural characteristics and properties of the regenerated silk fibroin prepared from formic acid. Int J Biol Macromol 2001;29:91-7.
8. Rizzo G, Lo Presti M, Giannini C, Sibillano T, Milella A, Guidetti G, *et al*. *Bombyx mori* silk fibroin regeneration in solution of lanthanide ions: A systematic investigation. Front Bioeng Biotechnol 2021;9:653033.
9. Inoue S, Tanaka K, Arisaka F, Kimura S, Ohtomo K, Mizuno S. Silk fibroin of *Bombyx mori* is secreted, assembling a high molecular mass elementary unit consisting of H-chain, L-chain, and P25, with a 6: 6: 1 molar ratio. J Biol Chem 2000;275:40517-28.
10. Yun H, Oh H, Kim MK, Kwak HW, Lee JY, Um IC, *et al*. Extraction conditions of *Antheraea mylitta* sericin with high yields and minimum molecular weight degradation. Int J Biol Macromol 2013;52:59-65.
11. Samie M, Muhammad N, Yameen MA, Chaudhry AA, Khalid H, Khan AF. Aqueous solution of a basic ionic liquid: A perspective solvent for extraction and regeneration of silk powder from *Bombyx mori* silk cocoons. J Polym Environ 2020;28:657-67.
12. Darshan GH, Kong D, Gautrot J, Vootla S. Physico-chemical characterization of *Antheraea mylitta* silk mats for wound healing applications. Sci Rep 2017;7:10344.
13. Rajkumar G, Srinivasan J. Characterization of recycled silk fiber PP composites with optimal performance of silk fibers by response surface methodology. J Test Eval 2018;48:3392-409.
14. Lee OJ, Kim JH, Moon BM, Chao JR, Yoon J, Ju HW, *et al*. Fabrication and characterization of hydrocolloid dressing with silk fibroin nanoparticles for wound healing. Tissue Eng Regen Med 2016;13:218-26.
15. Liu TL, Miao JC, Sheng WH, Xie YF, Huang Q, Shan YB, *et al*. Cytocompatibility of regenerated silk fibroin film: A medical biomaterial applicable to wound healing. J Zhejiang Univ Sci B 2010;11:10-6.
16. Xie C, Li W, Liang Q, Yu S, Li L. Fabrication of robust silk fibroin film by controlling the content of β-sheet via the synergism of Uv-light and ionic liquids. Appl Surf Sci 2019;492:55-65.
17. Hu D, Xu Z, Hu Z, Hu B, Yang M, Zhu L. pH-triggered charge-reversal silk sericin-based nanoparticles for enhanced cellular uptake and doxorubicin delivery. ACS Sustain Chem Eng 2017;5:1638-47.
18. Bhattacharjee M, Schultz-Thater E, Trella E, Miot S, Das S, Loparic M, *et al*. The role of 3D structure and protein conformation on the innate and adaptive immune responses to silk-based biomaterials. Biomaterials 2013;34:8161-71.
19. Lachkova V, Varbanov S, Hägele G, Keck H, Tosheva T. Urea and thiourea derivatives of bis (dimethyl-phosphinoylmethyl)-amine. Phosphorus Sulfur Silicon Relat Elem 2002;177:1303-13.
20. He Z, Zhao T, Zhou X, Liu Z, Huang H. Sequential order of the secondary structure transitions of proteins under external perturbations: Regenerated silk fibroin under thermal treatment. Anal Chem 2017;89:5534-41.
21. Lv L, Wei Y, Wang J, Li M, Zhao H, Liu G, *et al*. Preparation and physical properties of *Antheraea yamamai*/*Bombyx mori* silk fibroin blending film. In: Proceedings of the 2011 4th International Conference on Biomedical Engineering and Informatics (BMEI). Vol. 03. Shanghai, China: IEEE; 2011. p. 1245-50.
22. Zhang F, Yang R, Zhang P, Qin J, Fan Z, Zuo B. Water-rinsed nonmulberry silk film for potential tissue engineering applications. Acs Omega 2019;4:3114-21.
23. Li M, Tao W, Kuga S, Nishiyama Y. Controlling molecular conformation of regenerated wild silk fibroin by aqueous ethanol treatment. Polym Adv Technol 2003;10:694-8.
24. Li M, Tao W, Lu S, Kuga S. Compliant film of regenerated *Antheraea pernyi* silk fibroin by chemical crosslinking. Int J Biol Macromol 2003;32:159-63.
25. Kazemimostaghim M, Rajkhowa R, Patil K, Tsuzuki T, Wang X. Structure and characteristics of milled silk particles. Powder Technol 2014;254:488-93.
26. Muthumanickkam A, Subramanian S, Goweri M, Beaula WS, Ganesh V. Comparative study on eri silk and mulberry silk fibroin scaffolds for biomedical applications. Iran Polym J 2013;22:143-54.
27. Huo P, Ding H, Tang Z, Liang X, Xu J, Wang M, *et al*. Conductive silk fibroin hydrogel with semi-interpenetrating network with high toughness and fast self-recovery for strain sensors. Int J Biol Macromol 2022;212:1-10.
28. Maity B, Samanta S, Sarkar S, Alam S, Govindaraju T. Injectable silk fibroin-based hydrogel for sustained insulin delivery in diabetic rats. ACS Appl Bio Mater 2020;3:3544-52.
29. Castellano I, Merlino A, Castellano I, Merlino A. In: Butler P, editor. Springer Briefs in Biochemistry and Molecular Biology. Switzerland: Springer Basel; 2013.
30. Rockwood DN, Preda RC, Yücel T, Wang X, Lovett ML, Kaplan DL. Materials fabrication from *Bombyx mori* silk fibroin. Nat Protoc 2011;6:1612-31.
31. Rupesh D, Soumen M, Kundu SC. Isolation, purification and characterization of silk protein sericin from cocoon peduncles of tropical tasar silkworm, *Antheraea mylitta*. Int J Biol Macromol 2006;38:255-8.
32. Mejía-Suaza ML, Moncada ME, Ossa-Orozco CP. Characterization of electro spun silk fibroin scaffolds for bone tissue engineering: A review. TecnoLógicas 2020;23:49.
33. Motta A, Fambri L, Migliaresi C. Regenerated silk fibroin films: Thermal and dynamic mechanical analysis. Macromol Chem Phys 2002;203:1658-65.
34. Inoue K, Takei K, Denda M. Functional glycine receptor in cultured human keratinocytes. Exp Dermatol 2015;24:307-9.
35. Andiappan M, Kumari T, Sundaramoorthy S, Meiyazhagan G, Manoharan P, Venkataraman G. Comparison of eri and tasar silk fibroin scaffolds for biomedical applications. Prog Biomater 2016;5:81-91.

How to cite this article:
Dixit S, Gasti T, Sherapura A, Prabhakar BT, Vootla SK. Biocompatibility of hydrophilic regenerated *Antheraea mylitta* silk fibroin. J App Biol Biotech. 2023;11(4):164-169. DOI: 10.7324/JABB.2023.11512